Topological analysis of the ATP-gated ionotrophic $P2X_2$ receptor subunit

Gonzalo E. Torres, Terrance M. Egan, Mark M. Voigt*

Department of Pharmacological and Physiological Science, St. Louis University School of Medicine, St. Louis, MO 63104, USA

Received 20 January 1998; revised version received 16 February 1998

Abstract We investigated the transmembrane topology of the $P2X_2$ receptor subunit expressed in HEK 293 cells. Initial studies using two P2X subunits expressed in tandem indicated that the amino- and carboxy-termini are on the same side of the membrane. Immunofluorescence studies showed the cytoplasmic orientation of the amino- and carboxy-termini. Finally, *N*-glycosylation scanning mutagenesis revealed that reporter sites inserted into the central loop, but not those in the amino- or carboxy-terminal regions, were glycosylated, thus suggesting an extracellular placement for that domain. Our results support a two-transmembrane arrangement for P2X receptors with intracellular amino- and carboxy-termini.

Key words: P2X receptor; Adenosine triphosphate; Membrane topology; Glycosylation

1. Introduction

P2X receptors are non-selective cation channels activated by extracellular ATP [1]. These receptors, comprising a family of seven genes, are thought to be oligomeric in nature. Recent reports have demonstrated that the individual subunit proteins differ in a number of ways, ranging from their agonist binding profiles and biophysical properties [2–7] to their ability to form heteromeric assemblies [8]. Obviously, investigation into these varied properties of P2X receptors would be greatly aided by knowledge of the topography of these proteins.

Current models of P2X protein architecture are based on computer analysis of their primary sequences, which suggests that the N-termini are intracellular and that they contain only two transmembrane (TM) domains [2,3]. This is in marked contrast to what is known for other ligand-gated ion channels, such as the nicotinic cholinergic and ionotropic glutamate receptors which have extracellular N-termini and three or more transmembrane-spanning segments [9–14]. Although analyses of primary sequences are commonly used to predict the topology of membrane proteins [15,16], these protocols are useful only as a first step in the elucidation of the two-dimensional orientation of integral membrane proteins. This caveat has been amply demonstrated in the case of G-protein coupled receptors which do not contain consensus signal peptide sequences yet their N-termini are extracellular [17] and for ionotropic glutamate receptors that were predicted to have extracellular C-termini which in fact are intracellular [12–14]. Thus, it is extremely important to empirically determine the topology of these proteins and not to rely on computer analysis.

*Corresponding author. Fax: (1) (314) 577-8233.
E-mail: voigtm@slu.edu

In the case of P2X receptors, there is little information concerning the topological organization of the protein. Mutagenic studies have shown that two amino acids (aa) located on the putative extracellular loop of $P2X_4$ are critical for conferring sensitivity to the antagonist PPADS (pyridoxal-phosphate-6-azophenyl-2′,4′-disulfonic acid tetrasodium) [5,18]. The only biochemical evidence concerning the topology of P2X receptors is based on the finding that $P2X_1$ can be glycosylated in vitro [19]. The studies described above are restricted to a few aa located in the central loop and localization studies have not been reported for any other region of the protein. The aim of the present report is to provide a structural model of P2X receptors supported by definitive localization studies. This model is a crucial aid in the design of experiments investigating not only extracellular areas of the protein involved in such functions as ligand binding, but also intracellular domains that can interact with cytosolic proteins involved in regulatory and/or cellular domain targeting functions. In this study we present data, using a combination of approaches, that for the first time demonstrate the topological organization of P2X receptor subunits.

2. Materials and methods

2.1. DNA constructs

Rat $P2X_2$ cDNA was used as template for amplification. Mutagenesis was carried out using the PCR with Vent polymerase (New England Biolabs). Reaction mixtures were subjected to 32–34 cycles using the following sequence: 94°C for 20 s, 55°C for 30 s, 72°C for 1–3 min with an additional 7 min at 72°C to ensure complete extension. To construct the dimer $P2X_2/P2X_3$ cDNA, a stretch of 10 glutamine residues followed by a *Pst*I site was introduced by PCR at the 3′ end of $P2X_2$ preceding the stop codon. The rat $P2X_3$ subunit was used as a template to introduce the *Nsi*I and *Xho*I sites at the 5′ end adjoining the initiation codon and at the 3′ end following the stop codon respectively. The two PCR fragments were digested with *Eco*RI/*Pst*I and *Nsi*I/*Xho*I respectively, ligated together and subcloned into pRK-5 [20]. This yielded a construct containing an open reading frame of 879 aa; aa 1–472 are from $P2X_2$, aa 473–482 are the glutamine spacers, and aa 483–879 are $P2X_3$. For the epitope tagging experiments, synthetic oligonucleotides were designed to introduce the FLAG epitope sequence (DYKDDDDK) at the amino-terminus following the initiation Met ($P2X_2$NF), and at the carboxy-terminus followed by the stop codon ($P2X_2$CF) of the $P2X_2$ subunit. The three potential *N*-linked glycosylation sites N182, N239, and N298 of $P2X_2$ were mutated individually to glutamine (Q) by PCR-mediated overlapping extension using the $P2X_2$NF cDNA as a template (these constructs were designated $P2X_2$NFΔG3). Removal of all three potential *N*-linked glycosylation sites was performed in two steps. N-terminally epitope-tagged $P2X_2$NFΔG1 was used as a template to introduce the second mutation at aa position 239 as described. This PCR product was then utilized as a template to introduce the third mutation at aa position 298. This construct, termed $P2X_2$NFΔG, was then utilized as the basis for inserting *N*-glycosylation consensus sequences NXS/T into putative hydrophilic regions. Sites were selected in such a way that in most cases only a single mutation was required to generate the entire consensus site. Two *N*-glycosylation sequences were created simultaneously at the amino-terminal domain by sequentially introducing the C9N mutation, and the I22N and V24S mutations by

PII S0014-5793(98)00179-3

PCR. Mutations introduced in the central loop were Q206N and T300N, whereas those selected in the carboxy-terminus were P381N and A434N. All PCR fragments containing the desired mutations were digested with *Eco*RI and *Xho*I and subcloned into pRK-5 [20]. Mutations were verified by DNA sequencing with the dideoxynucleotide chain termination method, utilizing the T7 Sequenase kit (Amersham).

2.2. Cell culture and DNA transfection

Human embryonic kidney cells (HEK 293) were grown in Eagle's modified minimal essential medium (MEM) (Gibco BRL) supplemented with 10% fetal bovine serum, 50 U/ml penicillin, 50 μg/ml streptomycin, and 2 mM glutamine, and placed in a humidified atmosphere containing 5% CO_2 at 37°C. HEK 293 cells grown to 50–60% confluence on 35 mm culture dishes were transfected using lipofectamine.

2.3. Electrophysiological recordings

A suspension of transiently transfected cells was made by agitating the solution bathing the cells attached to the bottom of a single culture dish using a fire-polished Pasteur pipette. Whole cell current was recorded from single cells using an AxoPatch 200A amplifier and low resistance electrodes (0.5–2 MΩ). Holding voltage was −40 mV. Borosilicate recording pipettes were filled with the following intracellular solution (in mM): 140 CsCl, 10 tetraethylammonium-Cl, 5 EGTA, 10 HEPES, pH 7.3 with CsOH. The composition of the extracellular solution was (in mM): 150 NaCl, 1 $CaCl_2$, 1 $MgCl_2$, 10 glucose, 10 HEPES, pH 7.3 with NaOH. Drugs were applied by manually moving the electrode and attached cell into the line of flow of solutions exiting an array of inlet tubes lying side by side. Short applications (approximately 3 s) of agonists were accomplished by moving cells in a linear fashion from control solution through a drug-containing solution to another control solution.

2.4. Indirect immunofluorescence and confocal microscopy

Transiently transfected HEK 293 cells grown on glass coverslips were fixed with fresh 2% paraformaldehyde in phosphate-buffered saline (PBS) for 10 min. In some cases, cells were permeabilized with 0.05% Nonidet P-40 in PBS for 10 min at room temperature. Cells were then incubated for 1 h at room temperature in blocking solution (PBS, 1% bovine serum albumin, 5% goat serum) containing anti-FLAG M2 monoclonal antibody (mAb) (10 μg/ml, Kodak). After several washes with PBS, cells were incubated with diluted fluorescein isothiocyanate (FITC)-conjugated sheep anti-mouse (Sigma). The cells were then mounted in Vectashield (Vectorlabs) and analyzed using a MRC 1024 confocal laser scanning microscope (Bio-Rad).

2.5. Western blot analysis

HEK 293 cells grown on 35 mm culture plates were scraped into 100 μl of sodium dodecyl sulfate (SDS) sample buffer. Solubilized proteins were subjected to 12% SDS-polyacrylamide gel electrophoresis (SDS-PAGE), followed by transfer to Hybond (Amersham). The blots were incubated with 10 μg/ml of the FLAG-specific mAb M2 (Kodak) followed by peroxidase-conjugated sheep anti-mouse antibody (Amersham). Immunoreactivity was visualized by enhanced chemiluminescence using an ECL kit (Amersham) according to the manufacturer's instruction. For treatment with endoglycosidase H, solubilized proteins from transfected cells were incubated with 2 mU of endoglycosidase H (Boehringer Mannheim) at 30°C for 18 h. Samples were then analyzed by SDS-PAGE as described.

3. Results and discussion

The elucidation of the topography of the P2X subunit protein in the cell membrane is an important and necessary step toward identifying the structure of the ATP binding site, the domains involved in the formation of the channel pore, subunit assembly and the possible regulatory sites of the protein. As a first step in this process, we utilized a functional approach to investigate whether the amino- and carboxy-termini were localized to the same side of the membrane. To do so, we took advantage of the ability of these proteins to form homo- and hetero-oligomeric receptor assemblies. We hypothesized that if the amino- and carboxy-termini of a single P2X subunit are both on the same side of the membrane, two subunits placed in tandem as a single polypeptide would each be excepted to fold properly and be able to participate in the formation of functional receptor assemblies. If the two termini are not on the same side of the membrane, then the second subunit of the tandem would not fold properly because of the constraints placed on it by being covalently attached to the first subunit. Tandem channels have been employed successfully in a variety of contexts that include determination of membrane topology [21], subunit stoichiometry [22,23] and subunit positional effects [24]. Whether or not subunits on the same tandem both contribute to the same receptor assembly is not pertinent; what is important is the phenotype of the observed proteins. Previous studies have shown that the $P2X_2$ and $P2X_3$ subunits can co-assemble to form heteromeric channels that exhibit unique properties differing from either parent expressed as homomeric receptors. Homomeric $P2X_3$ receptors show strong desensitization in response to ATP and α,β-methylene-ATP (αβme-ATP), homomeric $P2X_2$ receptors are insensitive to αβme-ATP and show much less desensitization of ATP currents, whereas co-expression of the two results in a heteromeric channel with a non-desensitizing αβme-ATP current ([8] and Fig. 1). We therefore engineered a tandem cDNA which resulted in a chimeric protein containing a $P2X_2$ subunit linked to a $P2X_3$ subunit (designated $P2X_{2.3}$). We chose $P2X_3$ as the second subunit in the tandem to ensure that functional channels containing it would be sensitive to αβme-ATP. In this scenario, if only the first subunit in the tandem was folded properly and was functional, then any resulting receptors would have the homomeric $P2X_2$ phenotype and be insensitive to αβme-ATP (Fig. 1A). However, if the second subunit in the tandem was also folded properly,

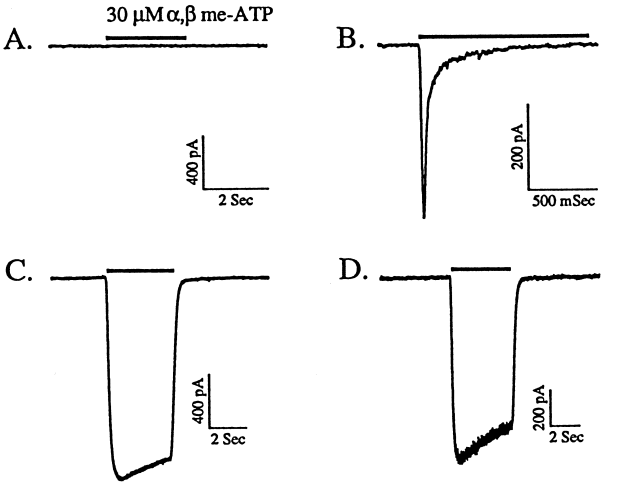

Fig. 1. αβme-ATP response in HEK 293 cells transfected with homomeric, heteromeric, and engineered tandem P2X subunits. Homomeric $P2X_2$ subunits are insensitive to the effect of αβme-ATP (A), whereas homomeric $P2X_3$ subunits show a strong desensitization in response to αβme-ATP (B). Co-expression of $P2X_2$ and $P2X_3$ subunits yields a receptor with a non-desensitizing αβme-ATP response (C). The $P2X_{2.3}$ tandem construct also gives a non-desensitizing αβme-ATP response (D) suggesting that both subunits are folded properly. Note: Cells transfected with wild-type $P2X_2$ gave a robust ATP response, confirming the presence of functional receptors (not shown).

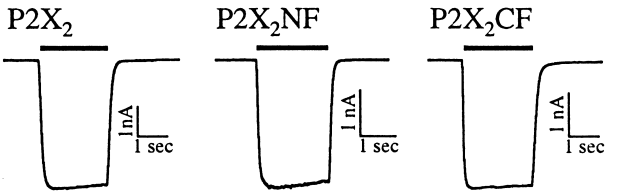

Fig. 2. ATP responses of wild-type and epitope-tagged $P2X_2$ receptor subunits. Recordings were obtained 24–48 h after HEK 293 cells were transfected with 1 μg of cDNA. The currents were elicited by 10 μM ATP from a holding potential of −40 mV. Traces are representative of at least three separate experiments.

then αβme-ATP-responsive receptors should be detected that exhibited a phenotype resembling either that of $P2X_3$ alone (Fig. 1B) or that of the heteromeric $P2X_2/P2X_3$ receptor (Fig. 1C). Demonstration of αβme-ATP sensitivity would therefore indicate that the second ($P2X_3$) subunit's N-terminus was on the same side of the membrane as the C-terminus of the first subunit ($P2X_2$). As shown in Fig. 1D, the $P2X_{2.3}$ tandem construct did indeed give a functional channel that exhibited a non-desensitizing current in response to αβme-ATP, and the time course of this response was similar to that observed with the heteromeric receptor formed by $P2X_2$ and $P2X_3$ subunits (Fig. 1). Such a finding can only be explained by the correct folding of both subunits present in the tandem. Thus, these results demonstrate that in functional P2X subunits the amino- and carboxy-termini must be located on the same side of the membrane.

We next used immunofluorescence combined with confocal microscopy to determine if the termini are intracellular or extracellular. To accomplish this, we first epitope-tagged the $P2X_2$ subunit by engineering the FLAG epitope into either the N-terminus ($P2X_2NF$) or C-terminus ($P2X_2CF$). The expression of homomeric $P2X_2NF$ or $P2X_2CF$ resulted in an ATP response resembling that of the wild-type $P2X_2$ (Fig. 2), indicating that these epitope-tagged subunits are capable of forming functional receptors. No detectable immunofluorescence was observed in untransfected HEK 293 cells or cells transfected with wild-type (untagged) $P2X_2$ subunits (data not shown). In the case of $P2X_2NF$ or $P2X_2CF$, the mAb M2 did not detect either of the tagged $P2X_2$ receptors at the membranes of non-permeabilized cells (Fig. 3A,C) but did in permeabilized cells (Fig. 3B,D), indicating that both the amino- and the carboxy-termini are intracellular in orientation. These findings are in line with other results from our laboratories that demonstrate the N-terminal portion of TM2 faces the extracellular space and that the C-terminal portion of TM2 resides intracellularly [25].

To investigate the membrane sideness of the entire protein, we utilized the fact that *N*-glycosylation of proteins occurs only on domains that are destined to be extracellular. Such an approach has been used successfully for topographic analysis of other channel proteins [13,14,26,27]. Analysis of the $P2X_2$ primary sequence indicates three potential *N*-linked glycosylation sites at aa positions 182, 239, and 299. To determine which, if any, of these sites are glycosylated, we removed each site individually from $P2X_2NF$. Western blot analysis of cells expressing the wild-type and glycosylation mutant $P2X_2NF$ subunits was then carried out using the anti-FLAG mAb M2. No bands were detected when the cells were transfected with the wild-type untagged $P2X_2$ (Fig. 4, lane 1). However, cells transfected with $P2X_2NF$ produced an *N*-glycosylated protein of approximately 70 kDa (Fig. 4,

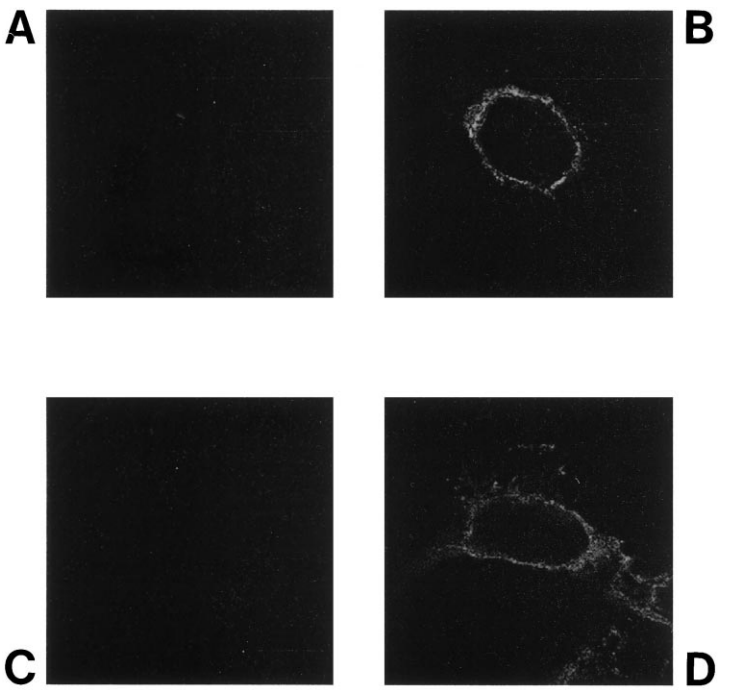

Fig. 3. Detection of epitope-tagged $P2X_2$ subunits by indirect immunofluorescence and confocal microscopy. HEK 293 cells expressing $P2X_2NF$ (A,B) or $P2X_2CF$ (C,D) were stained with M2 mAb under non-permeabilizing (left panels) and permeabilizing conditions (right panels). Cells were then incubated with fluorescein anti-mouse and subjected to immunofluorescence analysis using a Bio-Rad confocal microscope. The amino- and carboxy-termini of the tagged $P2X_2$ subunits were labeled only after permeabilization of the plasma membrane.

lane 2), as treatment with endoglycosidase H reduced the size of the protein to approximately 55 kDa (Fig. 4, lane 3). Removal of each of the three potential *N*-glycosylation sites did not alter ATP-induced currents in these receptors (data not shown), but did lead to an increase in the mobility of the mutant proteins as compared with $P2X_2NF$ (Fig. 4, lanes 4, 5, and 6). Moreover, when all three sites were removed from $P2X_2$ (designated $P2X_2NF\Delta G$), the protein was of a similar size to the endoglycosidase H-treated $P2X_2NF$ (Fig. 4, lane 7). These results indicate that each *N*-linked glycosylation site of $P2X_2$ is used in vivo and demonstrate that these residues are extracellular on functional proteins.

To confirm the intracellular orientation of the N- and C-termini, we used an *N*-glycosylation-linked scanning protocol in which we engineered *N*-glycosylation consensus sequences into putative intracellular and extracellular regions of $P2X_2NF$ and examined their accessibility to the glycosylation machinery. We used $P2X_2NF\Delta G$ as the parent construct so that *N*-glycosylation could only occur at the engineered sites, and we increased the chances of detecting glycosylation by inserting two consensus sequences. These sites were placed into one of three domains: the amino-terminus (preceding TM1, and designated $P2X_2NF\Delta G$-N), the central loop (designated $P2X_2NF\Delta G$-L), or the carboxy-terminal domain (following TM2, and designated $P2X_2NF\Delta G$-C). Fig. 5 shows the gel mobility shift analysis for the various scanning mutants. A decreased mobility was observed for $P2X_2NF\Delta G$-L compared to that of $P2X_2NF\Delta G$ (Fig. 5, lanes 2 and 4), indicating that the insertion of consensus sites at positions 206 and 300 in the central loop yielded a glycosylated receptor, and therefore further demonstrates the extracellular localization of this region. On the other hand, no glycosylation was observed when sites were inserted at positions 9 and 22 in the amino-terminus (Fig. 5, lane 3). Similar results were obtained when sites were inserted at positions 381 and 434 in the carboxy-terminus (Fig. 5, lane 5). These observations suggest that these sites were not available for glycosylation and therefore are intracellular.

In summary, the three independent sets of experiments presented in this report provide the first experimental evaluation of the topological model of P2X receptors deduced from hydropathy plots. Individually these strategies each have certain, but non-overlapping, limitations. For instance, insertion of epitopes or glycosylation consensus sequences might alter the secondary/tertiary properties of the protein and thus confound the interpretation of the results. Hence, the most compelling outcome of these various approaches would be that supported by convergent results. Indeed, such a conclusion was obtained in this study. The data are consistent with a two-transmembrane domain arrangement for P2X receptors with intracellular amino- and carboxy-termini and a large extracellular loop containing 10 positionally conserved cysteine residues. Although P2X receptors have no obvious primary sequence homology with other ligand-gated ion channels, the structural features described in this report are shared by an entirely different class of ion channels that include the amiloride-sensitive epithelial sodium channel [28], the FMRF-gated channel [29], and the mechanosensitive channel of *Caenorhabditis elegans* [30]. Our findings provide a starting point for the rational design of experiments aimed at elucidating the structural elements of P2X receptors that are involved in channel function and, by extension, in ATP-mediated intracellular signalling.

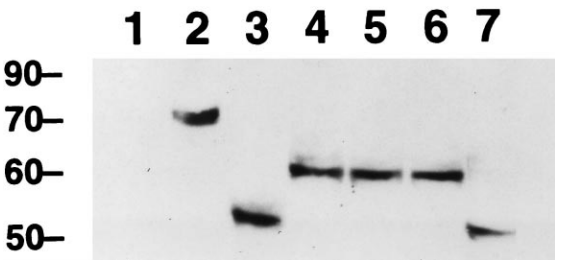

Fig. 4. *N*-Glycosylation at endogenous sites of $P2X_2$ as evidenced by electrophoretic mobility assay. Cell lysates expressing the different tagged $P2X_2$ *N*-glycosylation mutants were subjected to SDS-PAGE, electroblotted onto nitrocellulose, and incubated with anti-FLAG M2 mAb. Bands were detected with the ECL kit. Lane 1 represents the untagged control $P2X_2$, while lanes 2 and 3 show $P2X_2NF$LAG treated without and with endoglycosidase H, respectively. Lanes 4, 5, and 6 represent the three tagged mutants $P2X_2NF\Delta G1$–$P2X_2NF\Delta G3$ each lacking a single *N*-glycosylation site. Lane 7 represents the mutant $P2X_2NF\Delta G$, which lacks all three native *N*-glycosylation sites. Note the decreased mobility of the individual glycosylation mutants relative to the non-glycosylated $P2X_2$.

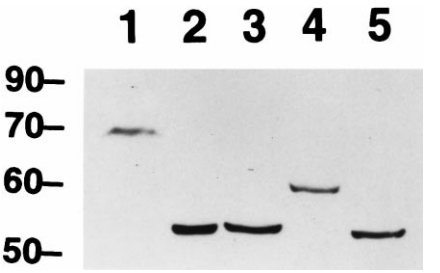

Fig. 5. *N*-Glycosylation of $P2X_2$ at engineered sites. HEK 293 cells were transfected with $P2X_2NF$LAG (lane 1), with non-glycosylated mutant $P2X_2NF\Delta G$ (lane 2) or with the engineered mutants: $P2X_2NF\Delta G$-N (lane 3), $P2X_2NF\Delta G$-L (lane 4), and $P2X_2NF\Delta G$-C (lane 5). After 48 h, lysates from transfected cells were subjected to SDS-PAGE and immunoblotting as described in the legend of Fig. 3. Note that the mobility of $P2X_2NF\Delta G$-N and $P2X_2NF\Delta G$-C is similar to that of $P2X_2NF\Delta G$.

Acknowledgements: We would like to thank Dr. D. Julius for providing the rat $P2X_2$ cDNA. We are also grateful to Dr. J. Cox for constructing the $P2X_{2.3}$ tandem cDNA, Drs. D. Lagunoff and R. Wysolmerski for assistance with the confocal microscopy, and Dr. P. Seguela for helpful discussions. This work was supported by NIH Grants NS35534 (M.M.V.) and HL56236 (T.M.E.).

References

[1] Fredholm, B.B., Abbracchio, M.P., Burnstock, G., Daly, J.W., Harden, T.K., Jacobson, K.A., Leff, P. and Williams, M. (1994) Pharmacol. Rev. 46, 143–156.
[2] Valera, S., Hussy, N., Evans, R.J., Adami, N., North, R.A., Surprenant, A. and Buell, G.N. (1994) Nature 371, 516–519.
[3] Brake, A.J., Wagenbach, M.J. and Julius, D. (1994) Nature 371, 519–523.
[4] Chen, C., Akopian, A.N., Sivilotti, L., Colquhoun, D., Burnstock, G. and Wood, J.N. (1995) Nature 367, 428–431.
[5] Buell, G., Lewis, C., Collo, G., North, R.A. and Surprenant, A. (1996) EMBO J. 15, 55–62.
[6] Collo, G., North, R.A., Kawashima, E., Merlo-Pich, E., Neidhart, S., Surprenant, A. and Buell, G. (1996) J. Neurosci. 16, 2495–2507.
[7] Surprenant, A., Rassendren, F., Kawashima, E., North, R.A. and Buell, G. (1996) Science 272, 735–738.

[8] Lewis, C., Neidhart, S., Holy, C., North, R.A., Buell, G. and Surprenant, A. (1995) Nature 377, 432–435.
[9] Barnard, E.A., Darlison, M.G. and Seeburg, P. (1987) Trends Neurosci. 10, 502–508.
[10] Devillers-Thiery, A., Galzi, J.L., Eisele, J.L., Bertrand, S., Bertrand, D. and Changeux, J.P. (1993) J. Membr. Biol. 136, 97–112.
[11] Karlin, A. (1993) Curr. Opin. Neurobiol. 3, 299–309.
[12] Tingley, W.G., Roche, K.W., Thompson, A.K. and Huganir, R.L. (1993) Nature 364, 70–73.
[13] Wo, Z.G. and Oswald, R.E. (1994) Proc. Natl. Acad. Sci. USA 91, 7154–7158.
[14] Hollman, M., Maron, C. and Heinemann, S. (1994) Neuron 13, 1331–1343.
[15] Kyte, J. and Doolittle, R.F. (1982) J. Mol. Biol. 157, 105–132.
[16] Eisenberg, D., Schwarz, E., Komaramy, M. and Wall, R.J. (1984) J. Mol. Biol. 179, 125–136.
[17] Venter, J.C., Karlavage, A.R. and Fraser, C.M. (1986) Biochem. Soc. Symp. 52, 1–22.
[18] Garcia-Guzman, M., Soto, F., Gomez-Hernandez, J.M., Lund, P. and Stuhmer, W. (1997) Mol. Pharmacol. 51, 109–118.
[19] Valera, S., Talabot, F., Evans, R.J., Gos, A., Antonarakis, S.E., Morris, M.A. and Buell, G.N. (1995) Receptors Channels 3, 283–289.
[20] Schall, T.J., Lewis, M., Koller, K., Lee, A., Rice, G.C., Wong, G.H.W., Gatanaga, T., Raab, H., Kohr, W.J. and Goeddel, D.V. (1990) Cell 61, 361–370.
[21] Blount, P., Sukharev, S.I., Moe, P.C., Schroeder, M.J., Guy, H.R. and Kung, C. (1996) EMBO J. 15, 4798–4805.
[22] Yang, J., Nung, Y.J. and Jan, L.Y. (1995) Neuron 15, 1441–1447.
[23] Silverman, S.K., Lester, H.A. and Dougherty, D.A. (1996) J. Biol. Chem. 271, 30524–30528.
[24] Paessia, M., Tucker, S.J., Lee, K., Bond, C.T. and Adelman, J.P. (1996) EMBO J. 15, 2980–2987.
[25] Egan, T.M., Haines, W.R. and Voigt, M.M. (1998) J. Neurosci. (in press).
[26] Chang, X., Hou, Y., Jensen, T. and Riordan, J.R. (1994) J. Biol. Chem. 269, 18572–18575.
[27] Hresko, R.C., Kruse, M., Strube, M. and Mueckler, M. (1994) J. Biol. Chem. 269, 20482–20488.
[28] Cannesa, C.M., Merillat, A.M. and Rossier, B.C. (1994) Am. J. Physiol. 267, 1682–1690.
[29] Linguelia, E., Champigny, G., Lazdunski, M. and Barpy, P. (1995) Nature 378, 730–733.
[30] Lai, C., Hong, K., Kinnel, M.C. and Driscoll, M. (1996) J. Cell Biol. 133, 1071–1081.